

Ultra-high-pressure shock-wave experiments

Charles E. Ragan III

Los Alamos Scientific Laboratory, University of California, Los Alamos, New Mexico 87545

(Received 2 October 1979)

The author has obtained Hugoniot data for uranium at a pressure of 6.7 TPa using a planar shock generated by an underground nuclear explosion. Measurements were made relative to a molybdenum standard in an impedance-matching experiment using 200-mm-diam by 20-mm-thick samples of each material. Twenty-seven electrical contact pins were used to measure shock velocities of 27.0 and 22.8 km/s ($\pm 1\%$) in the molybdenum and uranium, respectively; these velocities correspond to pressures and densities of 4.97 TPa and 30.8 g cm^{-3} (Mo) and 6.69 TPa and 59.0 g cm^{-3} (U). The measurement differs from a theoretical calculation by more than 2.5 times the experimental uncertainty and represents the highest pressure at which Hugoniot data have been obtained.

I. INTRODUCTION

In traditional laboratory experiments, shock-wave measurements have been limited to the pressure region well below 1 TPa. However, recent advances^{1,2} using laser-driven shocks indicate that this experimental limit may eventually be extended, but considerable development will be needed to achieve the required accuracy. At extremely high pressures (>30 TPa), theoretical treatments based on modified Thomas-Fermi (TF) statistical models³⁻⁵ are believed to represent material behavior reliably. However, in the intermediate-pressure region, calculations of material response under shock loading are uncertain since they are strongly influenced by such effects as atomic shell structure and pressure ionization; predictions of shock behavior have therefore relied upon various simplified models and extrapolations.

When a material is shocked from a given initial state, a point on its Hugoniot is reached, with pressure P , density $\rho = 1/V$, specific internal energy E , shock velocity D , and particle velocity u . Conservation laws relate the conditions on the two sides of the shock front and yield, in the steady state, the following equations (the Rankine-Hugoniot relations) in which the subscript 0 refers to the stationary material ahead of the shock:

$$\rho/\rho_0 = D/(D-u), \quad (\text{mass}),$$

$$P - P_0 \approx P = \rho_0 D u, \quad (\text{momentum}),$$

$$[(E - E_0) + \frac{1}{2}u^2]\rho_0 D = P u, \quad (\text{energy}).$$

Measurement of any two of the quantities (P, V, E, D, u) locates a point on the Hugoniot, which is a relation between P, V , and E :

$$E - E_0 = \frac{1}{2}(P + P_0)(V_0 - V).$$

However, direct determination of two parameters is especially difficult at high pressures, and impedance-matching experiments are often per-

formed in which measurements are made relative to a standard whose Hugoniot is known.

About ten years ago, we initiated an ultrahigh-pressure equation-of-state (EOS) program at the Los Alamos Scientific Laboratory, with our first goal being to provide experimental data for a standard material in this pressure region. As a first step in this program, we determined^{6,7} a point on the molybdenum Hugoniot at 2.0 TPa from direct measurements of both the shock velocity and the particle velocity. We chose molybdenum as our standard because of several physical properties. In addition, theoretical calculations were in good agreement with experiments at pressures up to ~ 0.25 TPa, and extension of these calculations to higher pressures were thought to present no unusual problems. This earlier experiment provided the first absolute measurement in this pressure region, and the excellent agreement with the theoretical predictions⁸ provided increased confidence in the calculated Hugoniot.

II. IMPEDANCE-MATCHING EXPERIMENTS

In impedance-matching experiments, Hugoniot data are obtained from measurements of shock velocities alone. In such relative experiments, the shock passes first through the standard material and then into an adjacent sample of the material under study, and the shock velocities D_i (standard) and D_x are determined, usually from position-versus-time measurements. For each material, the conservation of momentum relation and the measured shock velocity specify a straight line in the (P, u) plane with slope $\rho_0 D$. This quantity $\rho_0 D$, which is defined as the material impedance, is different for each material and shock strength; the intersection of the line $P = (\rho_0 D)_i u$ with the Hugoniot of the standard determines its pressure and particle velocity (P_i, u_i) .

When the shock reaches the material interface,

it propagates into the sample and simultaneously generates a backward-moving wave in the standard. This backward-moving wave is either a rarefaction or a second shock, depending upon the relative impedance of the two materials, and it changes the pressure P_i and particle velocity u_i so that both quantities are continuous across the interface. The new values (P_x, u_x) lie on the Hugoniot of the sample and are determined by the intersection of the straight line $P = (\rho_0 D)_x u$ with either the Hugoniot of the reflected shock (RS) or the release isentrope (RI) for the standard.

At low pressures, the curves RS and RI can be approximated by mirror reflections of the Hugoniot of the standard about a vertical line through the point (P_i, u_i) . This is no longer true at pressures of several TPa, and theoretical models must be used to calculate deviations away from this mirror Hugoniot. The corrections are not too severe, however, if the Hugoniot of the sample lies near that of the standard.

Several Soviet investigators⁹⁻¹³ have used lead as their standard in previous high-pressure impedance-matching experiments; calculations of the lead Hugoniot based on statistical theories were extrapolated from TF pressures into the intermediate pressure region, without the availability of experimental data. Recent modifications¹⁴ in their statistical treatment have resulted in changes in the calculated lead compression by 6-10% in the pressure region of interest, thus emphasizing the fact that knowledge of the Hugoniot of the standard is one of the largest uncertainties in impedance-matching experiments.

III. EXPERIMENTAL TECHNIQUE

In the present experiment, we used a planar, steady shock wave generated by an underground nuclear explosion to perform an impedance-matching experiment at higher pressures than in any previous measurements. The shock passed first through a lead base plate into the molybdenum standard and then into the depleted uranium (²³⁸U). The molybdenum and uranium disks were 200 mm in diameter by about 20 mm thick. The entire assembly was located approximately 3 m from the nuclear explosion and was well shielded from both neutrons and γ rays. The preshock energy deposited in the uranium, based on a detailed Monte Carlo calculation, increased its temperature < 300 K; much less energy was deposited in the other materials.

To determine both the shape of the shock front and its position as a function of time, 27 electrical contact pins were located at various positions in the sample assembly, as shown in Fig. 1. The pin

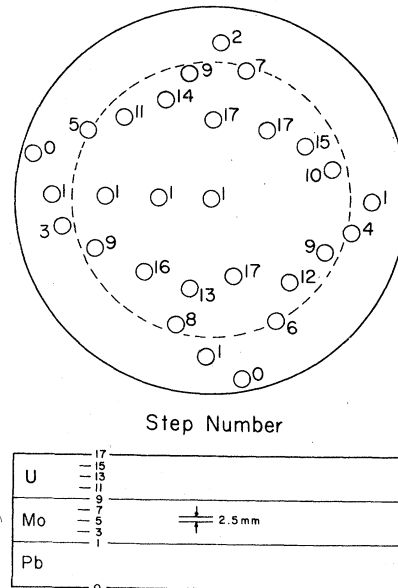


FIG. 1. Schematic of the sample assembly containing a lead base plate below disks of molybdenum and depleted uranium (²³⁸U). Also shown are the locations (see Table I) of the 27 electrical contact pins; their x , y positions are shown in the upper portion, with their z coordinates indicated in the lower part as a step number. In the molybdenum and uranium the steps were separated by approximately 2.5 mm, and only the odd-numbered ones are shown. The disks were approximately 200 mm in diameter by 20 mm thick; the dashed circle shows the region at the base of the uranium that was unperturbed by a rarefaction from the sample edge.

numbers refer to the step positions given in the lower portion. Similar pins had been successfully tested in previous experiments^{7,15}; each pin consisted of an aluminum center conductor surrounded by a 6.35-mm-o.d. insulating polycarbonate plastic (Lexan) rod, which was coated with a thin layer of copper. The center conductor was insulated from the lower end of the copper-clad Lexan rod by a 1-mm-thick Lexan plug. Shock arrival produced an electrical short between the charged center conductor and the grounded copper coating.

The pins were set at 18 different depths, with six pins at the base of the molybdenum (No. 1), three pins at the molybdenum-uranium interface (No.9), and two pins and an evacuated light pipe (No. 17) on the top surface of the uranium. In addition, two pins near the base of the lead (No. 0) were used to provide a fiducial signal. Pins on successive steps were placed nearly diametrically opposite each other to obtain a better measure of the shock profile. Each pin was also positioned so that it would not be affected by a rarefaction wave from the sample outer edge and so that a rarefaction from its base would not interfere with any other pin.

The pin center conductors were charged to either plus or minus 600 V, so that upon shock arrival each pin produced a rapidly rising pulse followed by a decay to the baseline. Nine cables were used to transmit the 27 pin signals to the recording station, with three pins multiplexed onto each 0.85-km-long cable. The pins in each set of three had different decay times and were chosen so that the expected closure sequence would produce well-separated pulses with alternate polarities—thus providing a unique signature for each pin.

IV. RESULTS AND CONCLUSIONS

Figure 2 shows representative signals from two of the cables. Each signal was recorded on a set of three or four oscilloscopes that were triggered sequentially to provide continuous, slightly overlapping coverage for about 4 μ sec. A time base, shown as the upper trace for each signal, was provided by 10-MHz time marks. The small, sharp initial pulse on each cable corresponds to a fiducial signal used to provide a common timing reference. The pin closure signals have rise times of ~ 17 nsec and are labeled by their corresponding step number. We have digitized each trace and the corresponding time marks by several independent readings. Based on these readings, we have obtained the arrival time at each pin with a standard deviation of < 2 nsec. After correcting for differ-

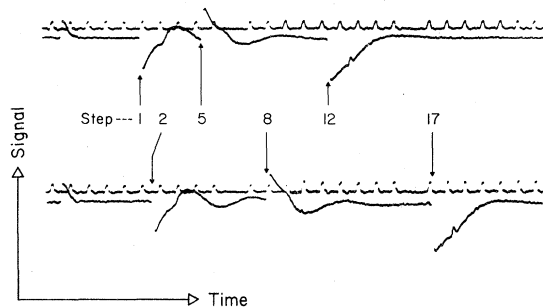


FIG. 2. Representative oscilloscope traces obtained from two of the signal cables, with pins at steps 1, 2, 5, 8, 12, 17 (see Fig. 1). For each cable, a set of three or four oscilloscopes was used to provide continuous coverage for about 4 μ sec. (These traces have been edited for clarity by combining three oscilloscope sweeps into each trace, but have not been corrected for differences in cable length.) The upper trace is a time base with a period of 100 nsec. At the beginning of the sweep of the first oscilloscope in each set, a fiducial marker was generated to provide common timing between the signal cables. Pin closures at shock arrival are labeled by their corresponding step numbers and are seen as rapid rises (~ 17 nsec) followed by slower returns to the base line, with the sequence of pin closures giving pulses of alternate polarity.

TABLE I. Pin coordinates and shock arrival times.

Step number	Pin coordinate (mm)			Arrival time (nsec) ^b
	<i>x</i>	<i>y</i>	<i>z</i> ^a	
1	0.0	0.0	0.0	1924.47
1	-23.800	0.0	0.025	1933.78
1	-47.219	0.0	0.025	1930.28
1	-70.637	0.0	0.030	1940.89
1	70.637	0.0	0.043	1936.63
1	0.0	-70.637	0.107	1922.63
2	0.0	69.063	2.418	2011.89
3	-65.888	-14.275	5.011	2098.29
4	63.678	-13.284	7.498	2184.61
5	-57.556	26.594	10.025	2270.07
6	30.556	-53.569	12.540	2374.64
7	13.462	58.293	15.034	2456.57
8	-13.081	-56.744	17.544	2555.41
9	-50.800	-24.206	20.020	2641.74
9	-13.106	54.864	20.020	2643.66
9	51.181	-23.012	20.028	2648.80
10	52.578	14.275	22.520	2760.13
11	-41.175	33.325	25.047	2855.94
12	35.306	-36.906	27.511	2971.53
13	-8.382	-40.386	30.043	
14	-22.733	42.062	32.512	3205.71
15	39.675	23.393	35.032	3320.33
16	-28.575	-33.731	37.541	3445.30
17	10.719	-34.519	40.010	3559.47
17	0.0	35.306	40.020	3566.06
17	23.800	30.150	40.000	3561.21 ^c

^a Distance from base of molybdenum.

^b Relative times measured from time ties on oscilloscope records.

^c Light-pipe arrival time. Includes correction of 28 nsec for transit across 1-mm-thick Lexan plug.

ing cable lengths and other delays in the recording system, we find that the relative uncertainty in each pin closure time is about ± 4 nsec.

Table I gives the x, y, z coordinates and arrival times for the pins, with the z coordinate specifying the distance from the base of the molybdenum disk. All but one of the pins functioned as expected, with the missing pin located at step 13. These data have been analyzed by fitting various functions to the x, y, z, t values for the 24 pins. We have obtained an upper limit to the tilt of 1.3 mrad by fitting the function $t = A + Bx + Cy + Dz + Ez^2$ to these data, with the requirements that dz/dx and dz/dy must have the same values in the two materials. This tilt introduces less than 3.3 nsec variation in arrival time along a radius. By including a term in either R or $R^2 = x^2 + y^2$ in the fitting function, we have concluded that nonplanar effects introduce less than 2.5-nsec delay in arrival at the edge relative to the center.

Figure 3(a) shows a plot of arrival time as a function of z in the molybdenum, and Fig. 3(b) shows a similar plot for the uranium. As is evi-

dent in these plots, the velocity decreased slightly as the shock moved through the samples. Therefore, we have used only the pins near both sides of the interface to determine the velocities. The solid lines in Fig. 3 represent least-squares fits of straight lines to these data and correspond to velocities of 27.0 km/s in the molybdenum and 22.8 km/s in the uranium. Based on these fits, the standard deviation in each point is 4 nsec, and the uncertainties in the slopes are $\pm 0.9\%$. We have assigned an overall uncertainty of $\pm 1\%$ to each velocity.

The shock arrival signal from the evacuated light pipe positioned on the upper surfaces of the uranium occurred ~ 30 nsec before the corresponding pin closure signals. However, the calculated transit time across the 1-mm-thick Lexan plug, based on several models of the Lexan EOS, is ~ 28 nsec. Thus the light-pipe signal is in excellent agreement with the pin signals. The pins at the interface were closed by a shock making a transition from molybdenum to Lexan. The pins

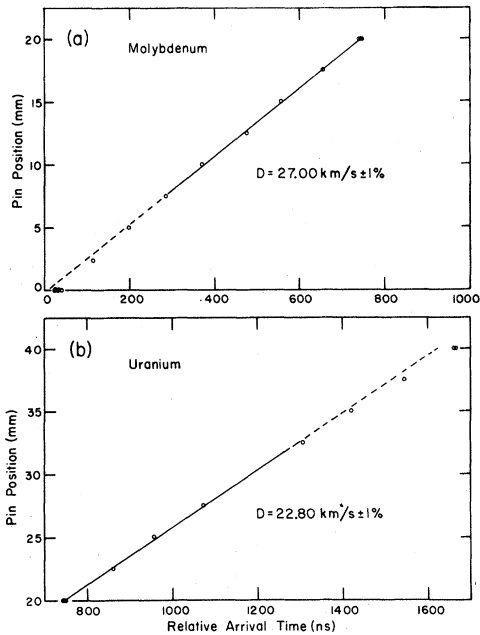


FIG. 3. Plots of the relative shock arrival time as a function of the pin distance from the base of the molybdenum (z coordinate in Table I). The solid straight lines are the results of least-squares fits to the data over the indicated intervals near the interface. The dashed portions are extensions of the lines and indicate a slight decrease in shock velocity with time. For the molybdenum (a) the indicated line corresponds to a shock velocity of 27.0 km/s, and for the uranium (b) the indicated line corresponds to a shock velocity of 22.8 km/s. The experimental uncertainties in these velocities are $\pm 1\%$.

in the uranium were closed by a shock transition from uranium to Lexan. This difference resulted in a 1.25-nsec-faster closure for the interface pins relative to the uranium pins. Thus, in making fits to the pin data for uranium, the arrival time at the interface was shifted by 1.25 nsec.

The measured shock velocities were used, with measured densities of 10.20 and 18.98 g cm^{-3} for molybdenum and uranium, respectively, to determine the straight lines plotted in the (P, u) plane in Fig. 4. The EOS for the molybdenum standard was taken from the SESAME library⁸ and included contributions to the pressure from the lattice, ions, and electrons. The measured shock velocity in molybdenum corresponds to a pressure of 4.97 TPa $\pm 2.3\%$, a particle velocity of 18.06 km/s $\pm 1.3\%$, and a density of 30.8 $\text{g cm}^{-3} \pm 0.5\%$. These uncertainties are due to experimental errors only,

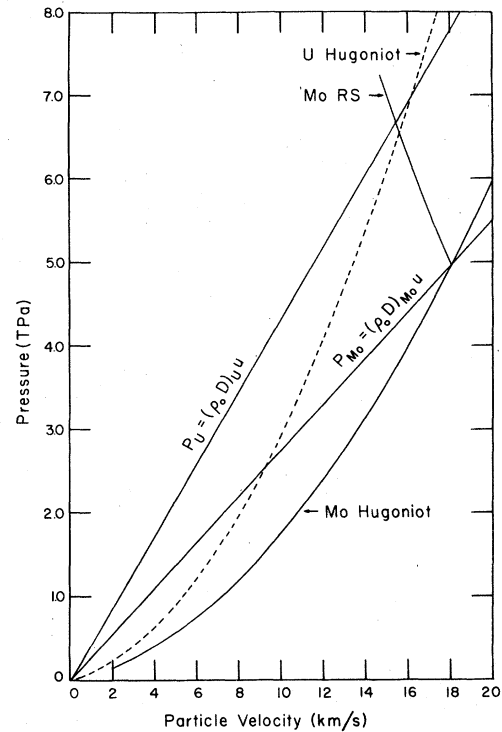


FIG. 4. Portion of the pressure-particle-velocity plane showing the pertinent curves used to determine a relative Hugoniot point for uranium by the impedance-matching technique. The straight lines were obtained from the measured shock velocities and have slopes of $(\rho_0 D)_{Mo}$ for molybdenum and $(\rho_0 D)_U$ for uranium. The line for molybdenum intersects the theoretical⁸ molybdenum Hugoniot at $P = 4.97 \text{ TPa} \pm 2.3\%$, $u = 18.06 \text{ km/s} \pm 1.3\%$. The Hugoniot of the reflected shock (RS) from this point intersects the experimentally determined straight line for uranium at $P = 6.69 \text{ TPa}$, $u = 15.46 \text{ km/s}$, a point that lies on the uranium Hugoniot. The dashed curve is the theoretical uranium Hugoniot from the SESAME library.⁸

and the small error in the density results from the correlation between the quantities D and $D - u$. The Hugoniot of the reflected shock based on the SESAME EOS intersects the straight line $P = \rho_0 Du$ for uranium to establish a Hugoniot point at a pressure of 6.69 TPa and a particle velocity of 15.46 km/s. The calculated Hugoniot for uranium from the SESAME library, however, intersects this straight line at a pressure of 6.99 TPa.

Figure 5 shows the 4–8 TPa region of the (P, u) plane plotted on an expanded scale. The rectangle is the region of uncertainty for the measured uranium Hugoniot point corresponding to 1% uncertainties in both shock velocities, which lead to uncertainties in the pressure and particle velocity of ± 2.3 and $\pm 2.1\%$, respectively. The density associated with this measured Hugoniot point [$\rho/\rho_0 = D/(D-u)$] is $59.0 \text{ g cm}^{-3} \pm 6.7\%$. Also shown is the

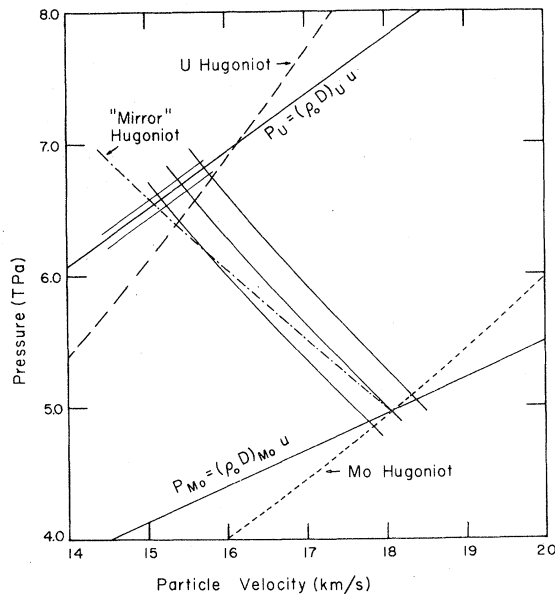


FIG. 5. Portion of the (P, u) plane plotted on an expanded scale (note depressed zeros). The shock state in the molybdenum lies on its theoretical Hugoniot (small dashes) at 4.97 TPa. The Hugoniot of the reflected shock originates here, and the two curves lying above and below this point correspond to uncertainties in the measured shock velocity of $\pm 1\%$. The straight line P_U is determined by the measured shock velocity in uranium, and the nearby parallel lines correspond to $\pm 1\%$ uncertainties. The rectangle represents the region of experimental uncertainty and corresponds to $P = 6.69 \text{ TPa} \pm 2.3\%$, $u = 15.46 \text{ km/s} \pm 2.1\%$. The region does not overlap the theoretical uranium Hugoniot (large dashes), which lies below the measured point and intersects the experimentally determined line P_U at a pressure of 6.99 TPa and a particle velocity of 16.16 km/s. The curve labeled "mirror" Hugoniot (dash-dot) corresponds to a reflection of the molybdenum Hugoniot about a vertical line through the point $P = 4.97 \text{ TPa}$, $u = 18.06 \text{ km/s}$.

"mirror" Hugoniot based on the initial shocked state in the molybdenum; it lies outside the error box. The SESAME Hugoniot point for uranium corresponds to a 2.6% larger shock velocity in the molybdenum or to a 2.8% smaller shock velocity in the uranium, both of which are well outside the experimental uncertainties.

The above uncertainties include only experimental errors of $\pm 1\%$ in the two shock velocities and do not include any uncertainties associated with errors in the theoretical molybdenum EOS. Obviously, the inclusion of such errors would increase the quoted uncertainties. Uncertainties in the theoretical molybdenum Hugoniot at 5.0 TPa are difficult to assess; our previous measurement^{6,7} for molybdenum increased our confidence in its calculated Hugoniot up to 2.0 TPa, and we hope to obtain other absolute high-pressure measurements for molybdenum with reduced errors. However, the present experiment does provide a check of the internal consistency of the models used to calculate Hugoniot for uranium and molybdenum. Since the theoretical molybdenum EOS is probably the more reliable of the two, the measurement indicates that the SESAME⁸ Hugoniot for uranium needs to be stiffer in this pressure region.

This is the first time that we have used the impedance-matching technique in this high-pressure region, and the quality of the data is excellent. The shock is untilted and planar, and we can readily avoid problems associated with the slight changes in velocity by utilizing only those points near the interface.

We are at present designing an experiment in which we hope to obtain data in this pressure region for a large number of samples relative to a molybdenum standard. In addition to obtaining shock-velocity measurements using electrical contact pins, we will test optical fibers as a means for detecting shock arrival in this high-radiation environment.

ACKNOWLEDGMENTS

An experiment of this kind is impossible without extensive support from many people. However, most important were the numerous valuable discussions with B. C. Diven, who was instrumental in starting this LASL high-pressure EOS program, and with M. G. Silbert. I wish to thank the Los Alamos Field Testing Division for their help in fielding the experiment, as well as W. J. Nellis, A. C. Mitchell, and M. J. Daddario (all of Lawrence Livermore Laboratory) for their initial help and suggestions about electrical contact pins. I also extend my thanks to W. A. Teasdale and

E. E. Robinson for their conscientious attention to the details associated with mechanical design and data recording. In addition, I am grateful to other members of the Neutron Physics Group (P-3) for their considerable efforts associated with the mechanical assembly. The efforts of M. Rich and R. B. Schultz, who provided hydrodynamical calcu-

lations necessary for designing the experiment, are also greatly appreciated. I also wish to thank J. C. Bozier, E. Genot, R. Vezin, and J. G. DiBona (all of Centre d'Etudes de Limeil) for valuable suggestions and discussions. This work was performed under the auspices of the U. S. Department of Energy.

-
- ¹L. R. Veaser and J. C. Solem, *Phys. Rev. Lett.* **40**, 1391 (1978).
- ²R. J. Trainor, J. W. Shaner, J. M. Auerbach, and N. C. Holmes, *Phys. Rev. Lett.* **42**, 1154 (1979).
- ³R. Latter, *Phys. Rev.* **99**, 1854 (1955); R. G. Cowan and J. Ashkin, *ibid.* **105**, 144 (1957).
- ⁴D. A. Kirzhnits, Yu. E. Lozovik, and G. V. Shpatakovskaya, *Sov. Phys. Usp.* **18**, 649 (1976).
- ⁵R. M. More, *Phys. Rev. A* **19**, 1234 (1979).
- ⁶C. E. Ragan III, M. G. Silbert, and B. C. Diven, *J. Appl. Phys.* **48**, 2860 (1977).
- ⁷C. E. Ragan III, M. G. Silbert, and B. C. Diven in *High Pressure Science and Technology*, edited by K. D. Timmerhaus and M. S. Barber (Plenum, New York, 1979), Vol. 2, p. 993; C. E. Ragan, in *Proceedings of the Symposium on Behavior of Dense Media Under High Dynamic Pressure* (Commissariat a l'Energie Atomique, Saclay, France, 1978), p. 477.
- ⁸B. I. Bennet, J. D. Johnson, G. I. Kerley, and G. T. Rood, Los Alamos Scientific Laboratory Report No. LA-7130, 1978 (unpublished); J. F. Barnes and G. T. Rood (private communication, 1973).
- ⁹L. V. Al'tshuler, B. N. Moiseev, L. V. Popov, G. V. Simakov, and R. F. Trunin, *Sov. Phys. JETP* **27**, 420 (1968).
- ¹⁰R. F. Trunin, M. A. Podurets, B. N. Moiseev, G. V. Simakov, and L. V. Popov, *Sov. Phys. JETP* **29**, 630 (1969).
- ¹¹M. A. Podurets, G. V. Simakov, R. F. Trunin, L. V. Popov, and B. N. Moiseev, *Sov. Phys. JETP* **35**, 375 (1972).
- ¹²R. F. Trunin, M. A. Podurets, G. V. Simakov, L. V. Popov, and B. N. Moiseev, *Sov. Phys. JETP* **35**, 550 (1972).
- ¹³R. F. Trunin, G. V. Simakov, M. A. Podurets, B. N. Moiseyev, and L. V. Popov, *Earth Phys.* **1**, 13 (1970).
- ¹⁴L. V. Al'tshuler, N. N. Kalitkin, L. V. Kuz'mina, and B. S. Chekin, *Sov. Phys. JETP* **45**, 167 (1977).
- ¹⁵C. E. Ragan III, M. G. Silbert, A. N. Ellis, E. E. Robinson, and M. J. Daddario, Los Alamos Scientific Laboratory Report No. LA-6946-MS, 1977 (unpublished).